IDENTIFICATION OF TRACTIONS BASED ON DISPLACEMENT OBSERVATIONS AT INTERIOR POINTS [1]

Masayuki NAKAJIMA, Ken HAYAMI, Jiro TERAO,
Seigo WATANABE* and Shigeru ANDO

Department of Mathematical Engineering and Information Physics
Graduate School of Engineering, University of Tokyo
7-3-1, Hongo, Bunkyo-ku, Tokyo, 113-8656 Japan
e-mail: *hayami@simplex.t.u-tokyo.ac.jp*
* Nissan Corporation, Yokosuka, Japan

ABSTRACT

This paper discusses the inverse problem of estimating the tractions on the boundary of an elastic body from displacement information observed at interior points. The problem arises, for instance, when estimating the tractions and the position where they are applied on the surface of a tactile sensor made of elastic body, from displacement observations obtained by ultrasonic cells inside the sensor body [1, 2]. We will formulate this inverse problem using the three-dimensional Boundary Element Method (BEM) and propose an algorithm to solve it. Finally, we will demonstrate the effectiveness of the algorithm through some numerical experiments.

KEYWORDS

Inverse Problem, Elastostatics, Boundary Element Method, Tactile Sensor, Generalized Inverse.

INTRODUCTION

Previous research on inverse analysis in elastostatics have mainly dealt with estimating unknown boundary quantities (displacement and/or traction) from over-specified boundary conditions for two-dimensional elasticity such as in [3] or [4]. In this paper we will deal with the inverse problem of identifying boundary tractions from displacement observations at internal points. Related work has been done in [5], where displacements on the boundary are estimated using displacement information at interior points using BEM for plane elasticity. The present work identifies concentrated tractions and the positions where they are applied on the boundary of a three-dimensional elastostatic body with the aim of

[1] Presented at ISIP 2000, International Symposium of Inverse Problems in Engineering, 7-10 March 2000, Nagano, Japan

applying it to tactile sensors [6, 7].

THE FORWARD PROBLEM

Let $\Gamma = \Gamma^{(N)} \cup \Gamma^{(D)}$ be the boundary of the region (elastic body) $\Omega \subset \mathbf{R}^3$, where traction is given on $\Gamma^{(N)}$ and displacement is given on $\Gamma^{(D)}$. Assume that Γ is discretized into boundary elements $\pi_i\,(1 \leq i \leq N)$. The boundary conditions for the forward problem (cf. Fig. 1) of determining the displacement at given interior (observation) points when tractions $\boldsymbol{\tau}_j\,(j = 1, ..., m')$ are applied at points $\boldsymbol{x}_j$ (boundary elements π_{n_j}) $(j = 1, ..., m')$ on $\Gamma^{(N)}$ is given as follows.

$$\begin{cases} \text{On } \pi_{n_j} \subset \Gamma^{(N)} \quad (\text{Representative position of } \pi_{n_j} : \boldsymbol{x}_{n_j}) & : \boldsymbol{t} = \boldsymbol{\tau}_j \quad (j = 1, ..., m'). \\ \text{On boundary elements in } \Gamma^{(N)} \text{other than } \pi_{n_j}\,(j = 1, ..., m') & : \boldsymbol{t} = \boldsymbol{0}. \\ \text{On elements in } \Gamma^{(D)} & : \boldsymbol{u} = \boldsymbol{0}. \end{cases}$$

Here, $\boldsymbol{t}$ and $\boldsymbol{u}$ are the traction and displacement on the boundary, respectively.

Solving this forward problem by the boundary element method, one first obtains the unknown traction on $\Gamma^{(D)}$ and unknown displacement on $\Gamma^{(N)}$. Then, the displacement at an arbitrary point in Ω can be determined.

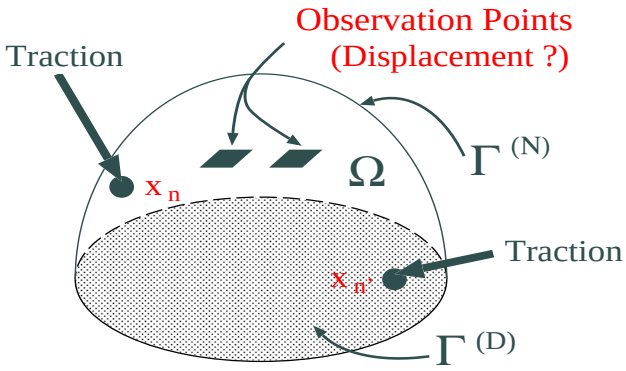

Figure 1: The forward problem.

THE INVERSE PROBLEM

Next, we will consider the corresponding inverse problem of estimating the tractions and the positions where they are applied on the boundary, from information of displacement at interior (observation) points.

The problem is not an imaginary one. For instance, in the tactile sensor made of elastic material proposed in [1, 2], the ultrasound displacement sensor imbedded in an elastic body detects the displacement at an interior point due to the contact traction on the surface of the elastic body with high precision. From this internal displacement information, the surface traction and its point of application must be estimated in real time.

The boundary and internal conditions for this inverse problem (cf. Fig.2) are given as

follows.

$$\begin{cases} \underline{\text{Boundary Condition}} & \\ \quad \text{On boundary elements in } \Gamma^{(N)} \text{ other than } \pi_{n_j}\ (j=1,...,m') & : \boldsymbol{t}=\boldsymbol{0}. \\ \quad\quad \text{where the tractions are applied} & \\ \quad \text{On boundary elements in } \Gamma^{(D)} & : \boldsymbol{u}=\boldsymbol{0}. \\ \underline{\text{Internal Condition}} & \\ \quad \text{At interior points } \boldsymbol{z}_i \in \Omega\ (i=1,\cdots,m) & : \boldsymbol{u}=\hat{\boldsymbol{u}}_i. \end{cases}$$

Here, $\hat{\boldsymbol{u}}_i$ denotes the given (observed) displacement at the internal point $\boldsymbol{z}_i$.

In this paper, we will formulate this problem using the boundary element method, and then propose an algorithm for the solution of the inverse problem.

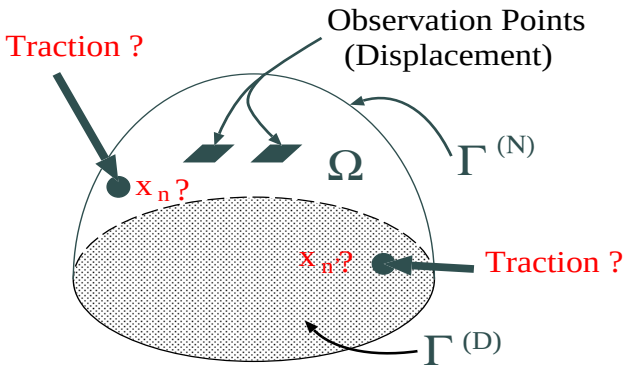

Figure 2: The inverse problem.

THE BOUNDARY ELEMENT FORMULATION OF THE FORWARD PROBLEM

The Boundary Integral Equation

The boundary integral equation for isotropic linear elastostatic materials is given by

$$\frac{1}{2}u_\alpha(\boldsymbol{x}) + \text{c.p.}\int_\Gamma t^*_{\alpha\beta}(\boldsymbol{x},\boldsymbol{y})u_\beta(\boldsymbol{y})\,\mathrm{d}\Gamma(\boldsymbol{y}) = \int_\Gamma u^*_{\alpha\beta}(\boldsymbol{x},\boldsymbol{y})t_\beta(\boldsymbol{y})\,\mathrm{d}\Gamma(\boldsymbol{y}) \quad (\alpha=1,2,3), \tag{1}$$

where the boundary Γ is assumed to be smooth at $\boldsymbol{x}$, and the body force has been neglected [8]. u_α and t_α are the displacement and traction components, respectively, and Einstein's summation convention for repeated indices are used. $u^*_{\alpha\beta}(\boldsymbol{x},\boldsymbol{y})$, $t^*_{\alpha\beta}(\boldsymbol{x},\boldsymbol{y})$ are the fundamental displacement and traction components, respectively.

Discretization Using Boundary Elements

The boundary Γ is then discretized into N planar boundary elements, and the boundary integral equation (1) is approximated as follows by the collocation method, where the displacement $\boldsymbol{u}$ and $\boldsymbol{t}$ are assumed to be constant on each element.

$$\frac{1}{2}u_\alpha(\boldsymbol{x}_i) + \text{c.p.}\sum_{j=1}^{N} u_\beta(\boldsymbol{x}_j)\int_{\Gamma_j} t^*_{\alpha\beta}(\boldsymbol{x}_i,\boldsymbol{y})\,\mathrm{d}\Gamma(\boldsymbol{y}) = \sum_{j=1}^{N} t_\beta(\boldsymbol{x}_j)\int_{\Gamma_j} u^*_{\alpha\beta}(\boldsymbol{x}_i,\boldsymbol{y})\,\mathrm{d}\Gamma(\boldsymbol{y})$$

$$(\alpha = 1,2,3, \quad i = 1,2,\cdots,N) \qquad (2)$$

Here, $\boldsymbol{x}_i$ is the node representing the i-th element. Let the 3×3 matrices $H_{ij} = (h_{ij\alpha\beta})$ and $G_{ij} = (g_{ij\alpha\beta})$, where

$$h_{ij\alpha\beta} = \int_{\Gamma_j} t^*_{\alpha\beta}(\boldsymbol{x}_i, \boldsymbol{y})\, \mathrm{d}\Gamma(\boldsymbol{y}), \qquad g_{ij\alpha\beta} = \int_{\Gamma_j} u^*_{\alpha\beta}(\boldsymbol{x}_i, \boldsymbol{y})\, \mathrm{d}\Gamma(\boldsymbol{y}),$$

and let I be the 3×3 identity matrix. Also let $\boldsymbol{t}_i = (t_\alpha(\boldsymbol{x}_i))$ and $\boldsymbol{u}_i = (u_\alpha(\boldsymbol{x}_i))$. Then, equation (2) can be written in matrix form as

$$\begin{bmatrix} \frac{1}{2}I + H_{11} & \cdots & H_{1N} \\ \vdots & \ddots & \vdots \\ H_{N1} & \cdots & \frac{1}{2}I + H_{NN} \end{bmatrix} \begin{bmatrix} \boldsymbol{u}_1 \\ \vdots \\ \boldsymbol{u}_N \end{bmatrix} = \begin{bmatrix} G_{11} & \cdots & G_{1N} \\ \vdots & \ddots & \vdots \\ G_{N1} & \cdots & G_{NN} \end{bmatrix} \begin{bmatrix} \boldsymbol{t}_1 \\ \vdots \\ \boldsymbol{t}_N \end{bmatrix}. \qquad (3)$$

Here, H_{ij} and G_{ij} are known quantities, and from the boundary condition of the forward problem, either $\boldsymbol{u}$ or $\boldsymbol{t}$ is given at each node. Hence, one can determine the unknown displacements and tractions from equation (3). That is, denoting the set of nodes with known displacement and unknown traction by 1, and the set of nodes with unknown displacement and known traction by 2, equation (3) can be rewritten as

$$\begin{bmatrix} \tilde{H}_{11} & \tilde{H}_{12} \\ \tilde{H}_{21} & \tilde{H}_{22} \end{bmatrix} \begin{bmatrix} \boldsymbol{U}_1 \\ \boldsymbol{U}_2 \end{bmatrix} = \begin{bmatrix} \tilde{G}_{11} & \tilde{G}_{12} \\ \tilde{G}_{21} & \tilde{G}_{22} \end{bmatrix} \begin{bmatrix} \boldsymbol{T}_1 \\ \boldsymbol{T}_2 \end{bmatrix},$$

where, for instance, $\boldsymbol{U}_1$ is the displacement vectors $\boldsymbol{u}(\boldsymbol{x})$ of the set of nodes 1 aligned in a column. Thus, we obtain the system of linear equations

$$\begin{bmatrix} \tilde{G}_{11} & -\tilde{H}_{12} \\ \tilde{G}_{21} & -\tilde{H}_{22} \end{bmatrix} \begin{bmatrix} \boldsymbol{T}_1 \\ \boldsymbol{U}_2 \end{bmatrix} = \begin{bmatrix} \tilde{H}_{11} & -\tilde{G}_{12} \\ \tilde{H}_{21} & -\tilde{G}_{22} \end{bmatrix} \begin{bmatrix} \boldsymbol{U}_1 \\ \boldsymbol{T}_2 \end{bmatrix},$$

and the unknown $\boldsymbol{T}_1$ and $\boldsymbol{U}_2$ are given by

$$\begin{bmatrix} \boldsymbol{T}_1 \\ \boldsymbol{U}_2 \end{bmatrix} = \begin{bmatrix} \tilde{G}_{11} & -\tilde{H}_{12} \\ \tilde{G}_{21} & -\tilde{H}_{22} \end{bmatrix}^{-1} \begin{bmatrix} \tilde{H}_{11} & -\tilde{G}_{12} \\ \tilde{H}_{21} & -\tilde{G}_{22} \end{bmatrix} \begin{bmatrix} \boldsymbol{U}_1 \\ \boldsymbol{T}_2 \end{bmatrix}, \qquad (4)$$

so that the displacement and traction at all the boundary nodes can be determined.

Computation of Displacement at an Interior Point

Similar to the boundary integral equation (1), the displacement at a point $\boldsymbol{z}$ interior to the region Ω is given by

$$u_\alpha(\boldsymbol{z}) + \int_\Gamma t^*_{\alpha\beta}(\boldsymbol{z}, \boldsymbol{y}) u_\beta(\boldsymbol{y})\, \mathrm{d}\Gamma(\boldsymbol{y}) = \int_\Gamma u^*_{\alpha\beta}(\boldsymbol{z}, \boldsymbol{y}) t_\beta(\boldsymbol{y})\, \mathrm{d}\Gamma(\boldsymbol{y}) \quad (\alpha = 1,2,3). \qquad (5)$$

Using the same discretization as in equation (2), equation (5) can be approximated by

$$u_\alpha(\boldsymbol{z}) + \sum_{i=1}^{N} u_\beta(\boldsymbol{x}_i) \int_{\Gamma_i} t^*_{\alpha\beta}(\boldsymbol{x}, \boldsymbol{z})\, \mathrm{d}\Gamma(\boldsymbol{x}) = \sum_{i=1}^{N} t_\beta(\boldsymbol{x}_i) \int_{\Gamma_i} u^*_{\alpha\beta}(\boldsymbol{x}, \boldsymbol{z})\, \mathrm{d}\Gamma(\boldsymbol{x}) \quad (\alpha = 1,2,3).$$

Defining the 3×3 matrices $H_i(\boldsymbol{z}) = (h_{i\alpha\beta}(\boldsymbol{z}))$ and $G_i(\boldsymbol{z}) = (g_{i\alpha\beta}(\boldsymbol{z}))$, where

$$h_{i\alpha\beta}(\boldsymbol{z}) = \int_{\Gamma_i} t^*_{\alpha\beta}(\boldsymbol{z}, \boldsymbol{y})\, \mathrm{d}\Gamma(\boldsymbol{y}), \qquad g_{i\alpha\beta}(\boldsymbol{z}) = \int_{\Gamma_i} u^*_{\alpha\beta}(\boldsymbol{z}, \boldsymbol{y})\, \mathrm{d}\Gamma(\boldsymbol{y}),$$

the displacement at the internal point $\boldsymbol{z}$ is approximated by

$$\boldsymbol{u}(\boldsymbol{z}) = [-H_1(\boldsymbol{z}) \ \cdots \ -H_N(\boldsymbol{z})] \begin{bmatrix} \boldsymbol{u}_1 \\ \vdots \\ \boldsymbol{u}_N \end{bmatrix} + [G_1(\boldsymbol{z}) \ \cdots \ G_N(\boldsymbol{z})] \begin{bmatrix} \boldsymbol{t}_1 \\ \vdots \\ \boldsymbol{t}_N \end{bmatrix}, \tag{6}$$

using the displacement and traction at each boundary node, which was given by equation (4).

ALGORITHM FOR THE INVERSE ANALYSIS

In [9], the three displacement components u_1, u_2, u_3 and $\dfrac{\partial u_3}{\partial x_1}$, $\dfrac{\partial u_3}{\partial x_2}$, $u_{rot} \equiv \dfrac{1}{2}\left(\dfrac{\partial u_2}{\partial x_1} - \dfrac{\partial u_1}{\partial x_2}\right)$ (six components altogether) at a single internal point were given as measured data, and an algorithm was proposed for the inverse analysis. In this paper, we will assume that the displacement components (u_1, u_2, u_3) are measured at more than one internal points.

Case when Traction is Applied at a Single Point

We will follow the argument in the previous section, with the traction $\boldsymbol{\tau}$ and its point of application on the boundary $\boldsymbol{x}_n$ unknown. In equation (4), all the unknown tractions and displacement vectors in $\boldsymbol{T}_1, \boldsymbol{U}_2$ can be expressed as affine transformations of $\boldsymbol{\tau}$. Moreover, since in our case, $\boldsymbol{u} = \boldsymbol{0}$ on $\Gamma^{(D)}$, and $\boldsymbol{t} = \boldsymbol{0}$ on $\Gamma^{(N)}$ except for π_n where $\boldsymbol{\tau}$ is applied, in fact $\boldsymbol{T}_1, \boldsymbol{U}_2$ can be expressed as linear transformations of $\boldsymbol{\tau}$. (Note that $\boldsymbol{u}(\boldsymbol{z}_i) = \boldsymbol{0}$.)

Hence, from equation (6), the displacement $\boldsymbol{u}(\boldsymbol{z}_i)$ at each internal observation point $\boldsymbol{z}_i$, $(i = 1, \cdots, m)$ can be expressed as a linear transformation of $\boldsymbol{\tau}$, that is

$$\boldsymbol{u}(\boldsymbol{z}_i) = A_i(\boldsymbol{x}_n)\boldsymbol{\tau},$$

where $A_i(\boldsymbol{x}_n)$ is a 3×3 matrix that does not depend on $\boldsymbol{\tau}$.

Thus, the applied traction $\boldsymbol{\tau}$ and the position $\boldsymbol{x}_n$ where it is applied on the boundary can be determined as the $\boldsymbol{\tau}$ and $\boldsymbol{x}_n$ which realize

$$\min_{\boldsymbol{\tau}, \boldsymbol{x}_n} \|\hat{\boldsymbol{u}} - \boldsymbol{u}\|^2. \tag{7}$$

Here, $\hat{\boldsymbol{u}}$ is the vector obtained by aligning the displacement vectors $\hat{\boldsymbol{u}}_i$ observed at the internal points $\boldsymbol{z}_i$ $(i = 1, \cdots, m)$ in a column, that is,

$$\hat{\boldsymbol{u}} = \begin{bmatrix} \hat{\boldsymbol{u}}_1 \\ \vdots \\ \hat{\boldsymbol{u}}_m \end{bmatrix}.$$

$\boldsymbol{u}$ is the vector obtained by aligning $\boldsymbol{u}(\boldsymbol{z}_i)$ vertically, that is,

$$\boldsymbol{u} = A(\boldsymbol{x}_n)\boldsymbol{\tau} = \begin{bmatrix} A_1 \\ \vdots \\ A_m \end{bmatrix} \boldsymbol{\tau}. \tag{8}$$

When $\boldsymbol{x}_n$ is fixed, A is a constant matrix whose column vectors are linearly independent. Thus, as in [9], the traction $\boldsymbol{\tau}$ which minimizes (7) is given, using the generalized inverse of A, by

$$\boldsymbol{\tau} = (A^{\mathrm{T}}A)^{-1}A^{\mathrm{T}}\hat{\boldsymbol{u}}. \tag{9}$$

Hence, equation (7) becomes

$$\min_{\boldsymbol{x}_{\mathrm{n}}} \|\{I - A(A^{\mathrm{T}}A)^{-1}A^{\mathrm{T}}\}\hat{\boldsymbol{u}}\|^2, \tag{10}$$

where we have used the matrix defined in equation (8), unlike in [9]. The $\tilde{\boldsymbol{x}}_n$ which minimizes equation (10) among all the position of the boundary elements $\boldsymbol{x}_n (1 \leq n \leq N)$ in $\Gamma^{(N)}$, is the position where the traction is applied, which was to be determined. Substituting this $\tilde{\boldsymbol{x}}_n$ in equation (10), we obtain the traction $\tilde{\boldsymbol{\tau}}$ which was also to be determined.

Case when Tractions are Applied at More than One Points

When tractions are applied at more than one points, a similar procedure can be performed. Assume that m' tractions $\boldsymbol{\tau}_j$ $(j = 1, \cdots, m')$ are applied at unknown positions $\boldsymbol{x}_{n_j}$ on the boundary. Then, from equation (4), all the unknown quantities on the boundary can be expressed as a sum of linear transformations of $\boldsymbol{\tau}_j$. Hence, from equation (6), the displacement $\boldsymbol{u}(\boldsymbol{z}_i)$ at each observation point $\boldsymbol{z}_i$ $(i = 1, \cdots, m)$ can be expressed as a sum of linear transformations of $\boldsymbol{\tau}_j$, that is,

$$\boldsymbol{u}(\boldsymbol{z}_i) = \sum_{j=1}^{m'} A_{ij}(\boldsymbol{x}_{n_j})\boldsymbol{\tau}_j\,, \tag{11}$$

where $A_{ij}(\boldsymbol{x}_{n_j})$ is a 3×3 matrix which does not depend on $\boldsymbol{\tau}_j$. Hence, the applied tractions $\boldsymbol{\tau}_j$ and their respective positions $\boldsymbol{x}_{n_j}$ $(j = 1, \cdots, m')$ where they are applied on the boundary are those that realize

$$\min_{\boldsymbol{\tau}_j, \boldsymbol{x}_{n_j}} \|\hat{\boldsymbol{u}} - \boldsymbol{u}\|^2. \tag{12}$$

Here, $\hat{\boldsymbol{u}}$ is the vector obtained by aligning the observed internal displacements in a column. $\boldsymbol{u}$ is the vector obtained by aligning $\boldsymbol{u}(\boldsymbol{z}_i)$ of equation (11) in a column, that is,

$$\boldsymbol{u} = \sum_{j=1}^{m'} A(\boldsymbol{x}_{n_j})\boldsymbol{\tau}_j = \sum_{j=1}^{m'} \begin{bmatrix} A_{1j} \\ \vdots \\ A_{mj} \end{bmatrix} \boldsymbol{\tau}_j = \begin{bmatrix} A_{11} & A_{12} & \cdots & A_{1m'} \\ A_{21} & A_{22} & \cdots & A_{2m'} \\ \vdots & \vdots & \ddots & \vdots \\ A_{m1} & A_{m2} & \cdots & A_{mm'} \end{bmatrix} \begin{bmatrix} \boldsymbol{\tau}_1 \\ \boldsymbol{\tau}_2 \\ \vdots \\ \boldsymbol{\tau}_{m'} \end{bmatrix}.$$

Next, let

$$A = \begin{bmatrix} A_{11} & A_{12} & \cdots & A_{1m'} \\ A_{21} & A_{22} & \cdots & A_{2m'} \\ \vdots & \vdots & \ddots & \vdots \\ A_{m1} & A_{m2} & \cdots & A_{mm'} \end{bmatrix}, \quad \boldsymbol{\tau}' = \begin{bmatrix} \boldsymbol{\tau}_1 \\ \boldsymbol{\tau}_2 \\ \vdots \\ \boldsymbol{\tau}_{m'} \end{bmatrix},$$

and fix all the positions $\boldsymbol{x}_{n_j}$ where the tractions are applied. Then, since A is a constant matrix whose column vectors are linearly independent as in equation(8), the tractions $\boldsymbol{\tau}'$ which minimize equation (12) is given using the generalized inverse of A as

$$\boldsymbol{\tau}' = (A^{\mathrm{T}}A)^{-1}A^{\mathrm{T}}\hat{\boldsymbol{u}}. \tag{13}$$

Hence, equation (12) can be rewritten as

$$\min_{\boldsymbol{x}_{n_j}} \|\{I - A(A^{\mathrm{T}}A)^{-1}A^{\mathrm{T}}\}\hat{\boldsymbol{u}}\|^2. \tag{14}$$

The positions $(\tilde{\boldsymbol{x}}_{n_1}, \tilde{\boldsymbol{x}}_{n_2} \cdots, \tilde{\boldsymbol{x}}_{n_{m'}})$ which minimizes equation (14) among all combinations for choosing m' elements from all the boundary elements in $\Gamma^{(N)}$, are the positions where the tractions are applied.

Evaluating equation (13) for these $(\tilde{\boldsymbol{x}}_{n_1}, \tilde{\boldsymbol{x}}_{n_2} \cdots, \tilde{\boldsymbol{x}}_{n_{m'}})$ gives the applied tractions at these points.

NUMERICAL EXPERIMENTS

The above algorithms for the inverse analysis were implemented for the three-dimensional problem, and numerical experiment results will be presented in order to demonstrate the effectiveness of the algorithm.

The experiment model is a hemisphere of radius 22mm made of elastic material (silicon rubber) with Young's modulus 5.0×10^6 Pa and Poisson's ratio near 0.5, just as in the actual tactile sensor proposed in [1, 2]. The base of the hemisphere is fixed (no displacement) and tractions are applied at some points on the hemisphere.

For the boundary element discretization of the model, 8 elements along the radius of the base of the hemisphere, 16 elements along the longitude and 8 elements along the latitude of the hemisphere were taken, resulting in 64 elements on the base and 128 elements on the hemisphere with a total of 192 elements, and the node of each element was taken at the centre of each element, as shown in Fig.3.

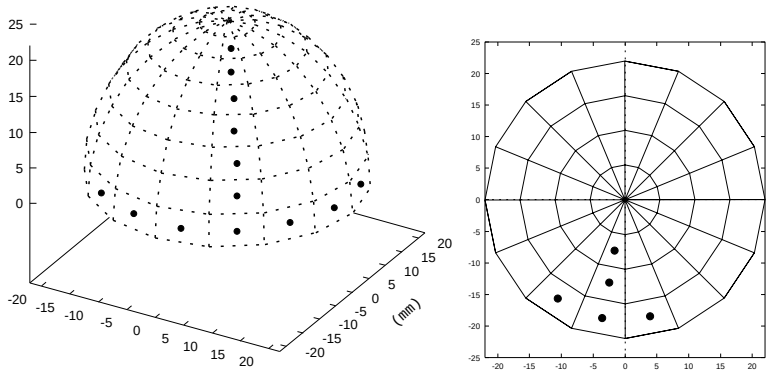

Figure 3: Boundary element discretization (left : hemispherical surface, right : base), where the points denote the nodes.

Case when Traction is Applied at a Single Point

The numerical experiment was done as follows. First, the forward problem was computed for a point traction of magnitude 300 Pa and arbitrary direction applied at some

point on the hemisphere. The displacements caused by this traction at several (two or four) internal points were then computed. The coordinates of the internal points were:

(Case of 2 internal points)$\cdots$ $(1,1,17),(-1,-1,17)$,
(Case of 4 internal points)$\cdots$ $(1,1,17),(-1,-1,17),(1,-1,17),(-1,1,17)$ (unit: mm),

reflecting feasible positions for placing the ultra sound cells for displacement measurements in the actual tactile sensor. The magnitude of the resulting displacements at the internal points were O(1)mm.

Then, for the inverse problem, 'measurement' errors of either $O(10^{-5})$mm, $O(10^{-3})$mm or $O(10^{-2})$mm were added to the displacement results obtained by the forward analysis, and then the inverse problem of estimating the applied traction was solved using the proposed algorithm. The same experiment was done, changing the position $\boldsymbol{x}_n$ where the traction $\boldsymbol{\tau}$ was applied.

As a result, when the error of the displacement measurement was $O(10^{-5})$mm or $O(10^{-3})$mm, the position where the traction was applied was correctly estimated, and the relative error of the estimated traction (size and components) were $O(10^{-5})$ and $O(10^{-3})$, respectively, whether the number of internal points for displacement measurement were two or four. This is reasonable, since the number of unknowns for the traction and its position is six altogether, which can be matched by the number of components of the displacement information for two internal points.

Fig.4 shows the relative error of the estimated traction as the latitude of the position where the traction was applied changed, with the longitude fixed. Displacement was given at two interior points with 'measurement' error of $O(10^{-3})$mm. The relative error of the estimated traction size and x, y, z components were derived by dividing the respective absolute error by the size of the traction. The relative error of the estimated traction is seen to be $O(10^{-3})$.

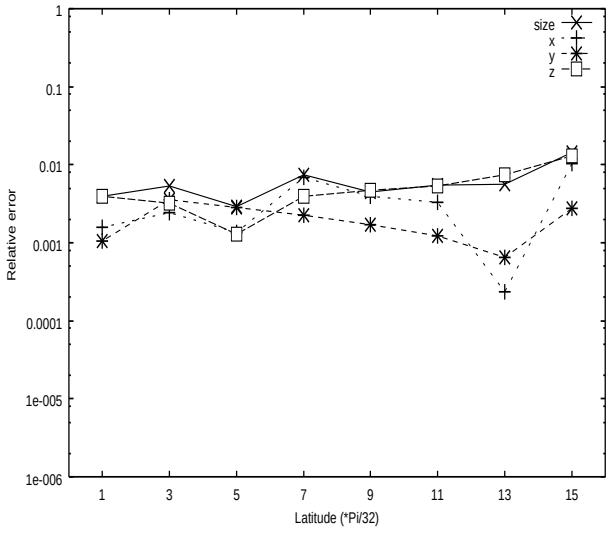

Figure 4: Case when traction is applied at a single point. (Relative error of estimated traction vs. Latitude of the position where the traction is applied. Two interior points for displacement measurement with error: $O(10^{-3})$mm.)

When the error of the displacement measurement was $O(10^{-2})$mm, the estimated position of the traction $\tilde{\boldsymbol{x}}_n$ was different from the true position, and the estimated traction

$\tilde{\boldsymbol{\tau}}$ was far from the true traction, whether the number of internal points for displacement measurement were two or four. In practice, the usual resolution of the sensor for displacement measurement embedded in the tactile sensor in [1, 2, 9] is $O(10^{-2})$mm for each displacement component (u_x, u_y, u_z), and it takes a long time to improve that resolution to $O(10^{-3})$mm by taking averages over a large number of measurements.

Therefore, we still need to improve the inverse analysis for the case when the error of the displacement measurement is $O(10^{-2})$mm. This may be done by using regularization techniques, refining the discretization, or optimizing the position of the internal points for displacement measurement.

The computations were done on a 200MHz PC. The precomputation for the matrix set up took 19 seconds, while the actual search for the inverse analysis took only one second, which is sufficiently small for real-time application.

Case when Tractions are Applied at Two Points

Next, we will test the inverse algorithm for the case when two tractions are applied on the same hemispherical model. This time, displacement measurements are given at four interior points, which are now necessary to identify the two tractions and the points where they are applied.

Similar to the previous case, 'measurement errors' are added to the forward analysis results, and the measurement accuracy required to identify the position of the two tractions will be observed. The size of the two tractions are 300 Pa, and the directions of the tractions are taken at random. The position where one of the tractions is applied is fixed at longitude= $\pi/16$ and latitude= $13\pi/32$ radians. The position of the other traction is varied.

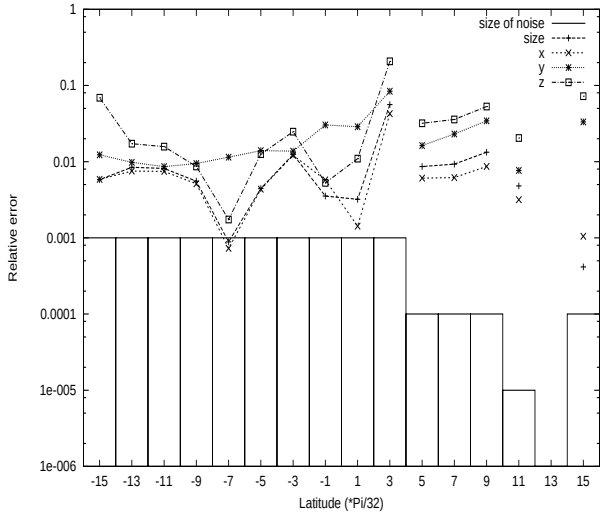

Figure 5: Case when tractions are applied at two points. (Lines: Relative error of the estimated tractions, Bar: Necessary precision (mm) for the displacement measurement at the internal points vs. Latitude of the position where the second traction is applied. Four interior points for displacement measurement.)

In Fig. 5, the relative error of the estimated traction (size and x, y, z components) are shown in lines, and the necessary precision (mm) for the displacement measurement at the internal points is shown in bars, as the latitude of the position where the second traction is applied is varied. For most positions, the position of the two tractions are correctly estimated and the relative error of the estimated traction is $O(10^{-2})$ if the measurement precision for the internal displacement is $O(10^{-3})$mm. However, more precision is required when the two points where the tractions are applied are close together. In this case the inverse analysis is ill-posed and regularization is required.

This time, the computation time for the exact search in the inverse analysis was 160 seconds, since the total number of combinations for the positions where two tractions are applied is significantly larger than for one. Heuristic iterative algorithms were attempted to reduce the number of searches without success. This was because the optimization problem for equation (14) has many local minimums. Therefore, a more efficient implementation of the exact search algorithm is required to speed-up the process so that it may be used in real-time application.

CONCLUSIONS

In this paper, we proposed an inverse algorithm using the boundary element method for estimating tractions and the position where they are applied on the boundary of a three-dimnsional elastic body, from information of displacement at internal points of the body caused by the tractions.

Numerical experiments for a model tactile sensor showed that for a single traction, when the measurement error of the internal displacement is less than $O(10^{-3})$mm, the applied traction and its position can be estimated with sufficient accuracy, with two internal points for displacement measurement. However, when the measurement error of the internal displacement was $O(10^{-2})$mm, the estimation was not satisfactory, and one needs to improve the inverse analysis using regularization techniques, refinement of the mesh, or optimization of the position of the internal points for measuring the displacements, etc.

For the case when tractions are applied at two points, similar results were obtained, although more measurement precision is required when the points are close together. The search for the inverse analysis also needs to be made more efficient for this case.

REFERENCES

[1] Naruse, M., Tamayama, K., Shinoda, H., and Ando, S., (1994) A 3-D structure tactile sensor based on ultrasonic deformation detection, *Proc. 33rd Conf. of SICE*, pp. 123–124, (in Japanese).

[2] Morohashi, T., Imai, R., Muramatu, G. and Ando, S., (1996) Integrated passive and active ultrasonic tactile sensor based on ultrasonic sensor, *Technical Digest of the 14th Sensor Symposium*, pp. 109–112.

[3] Dennis, B.H. and Dulikravich, G.S., (1998) A finite element formulation for the detection of boundary conditions in elasticity and heat conduction, *Inverse Problems in Engineering Mechanics*, Proc. Int. Symp. on Inverse Problems in Engineering Mechanics 1998 (ISIP'98), March, 1998, Nagano, pp. 61–70.

[4] Kubo, S. and Kawaguchi, M., (1998) A mathematical and numerical study on regularization of an inverse boundary value problem in elasto-static field, *Inverse Problems in Engineering Mechanics*, Proc. Int. Symp. on Inverse Problems in Engineering Mechanics 1998 (ISIP'98), March, 1998, Nagano, pp. 353–361.

[5] Ohura, Y., Kobayashi, K. and Onishi, K., (1998) Identification of boundary displacements in planar elasticity by BEM, *Engineering Analysis with Boundary Elements*, Vol. 20, No. 4, pp327–335.

[6] Nakajima, M., Watanabe, S., Hayami, K., (1999) Inverse analysis of an elastostatic problem, *Proc. 1999 Anual Meet. of JSIAM*, pp. 104–105, (in Japanese).

[7] Nakajima, M., Terao, J., Watanabe, S., Ando, S. and Hayami, K., (1999) Identification of traction based on displacement observations at interior points in an elastic body, *Proc. 16th Japan National Symp. on Boundary Element Methods*, JASCOME, pp. 103–108, (in Japanese).

[8] Brebbia, C.A., and Dominguez, J., (1992) *Boundary Elements An Introductory Course*, Second Edition, Computational Mechanics Publications, Southampton and McGraw-Hill Book Company, New York.

[9] Terao, J., Abe, M., and Ando, S., (1999) Application of the boundary element method to traction inversion problems of tactile sensor, *Proc. 38th Conf. of SICE*, pp. 343–344, (in Japanese).